Journal of Applied Polymer Science

Curing of poly(furfuryl alcohol) resin catalyzed by a homologous series of dicarboxylic acid catalysts: Kinetics and pot life

R. Marefat Seyedlar, M. Imani, S. M. Mirabedini
Iran Polymer and Petrochemical Institute, P.O. Box 14965-115, Tehran, Iran
Correspondence to: M. Imani (E-mail: m.imani@ippi.ac.ir)

ABSTRACT: Curing kinetics and pot life are two vital characteristics for the application of poly(furfuryl alcohol) (PFA) resin because of the complexities both in the resin composition and curing mechanisms involved. However, few reports have provided a complete picture of PFA curing behavior. In this research, the effect of the addition of catalysts on the pot life and curing behavior of a PFA resin were evaluated. A homologous series of dicarboxylic acids [i.e., oxalic acid (OX), succinic acid (SU), and adipic acid (SA)] were used as the catalysts. Rheometric and nonisothermal differential scanning calorimetry (DSC) measurements and headspace gas chromatography/mass spectrometry analysis were carried out at 0, 6, and 24 h after the addition of the catalyst. The relaxation exponent (n), gel stiffness (S), and gel strength (A_F) of the prepared compositions were calculated with the Winter and Chambon and Gabriele rheological models. Furthermore, the curing kinetics were evaluated by the fitting of nonisothermal, multiple-heating-rate models. The DSC measurements showed a higher curing degree for samples containing OX catalyst compared to their counterparts containing either SU or AD. The rheometric findings supported an increased stiffness, gel strength, and curing development of the resin in the presence of OX compared to samples containing SU or AD. © 2016 Wiley Periodicals, Inc. J. Appl. Polym. Sci. **2016**, *133*, 44009.

KEYWORDS: curing kinetics; differential scanning calorimetry (DSC); furan resin; pot life; rheometry

Received 16 February 2016; accepted 3 June 2016
DOI: 10.1002/app.44009

INTRODUCTION

Many research trials on polymer science and technology have been based on petroleum-derived monomers and polymers. Nevertheless, the continuous use of fossil raw materials in the years ahead will result in a drastic depletion of these reserves.[1] Furan (C_4H_4O) is the simplest oxygen-containing aromatic hydrocarbon, and its derivatives, including furfural and furfuryl alcohol (FA), are derived from the acid-catalyzed hydrolysis of pentosan-rich biomass (e.g., bagasse, oat hulls, corn husks, rice, and wheat straw) through dehydration and the cyclization of the ensuing pentoses.[2,3] Furfural, which is an aldehyde furan derivative,[3,4] is reduced to FA on a large scale.[5,6] Hence, these monomers which can be constantly regenerated by photosynthesis are abundantly available for the production of furan monomers resins. The fabrication of chemicals from such renewable resources is now important to a sustainable economy. Moreover, these materials can provide original polymer structures not readily available from petroleum-based chemistry.[4,5,7]

Materials derived from FA have been used in a wide range of industrial applications, most especially in the making of foundry cores and molds, the formulation of anticorrosion materials and intumescent coatings, the fabrication of graphitic compositions after pyrolysis, and use as adhesives, and coatings.[8,9] This has turned FA and its related products into some of the most important furanic materials available on the market. Poly(furfuryl alcohol) (PFA) resins have found widespread commercial applications where a high heat stability; acid, alkali, and solvent resistance; and a low flammability (with low smoke release) are needed at an affordable cost.[7,9] Furthermore, PFA resin is preferred over some other resins (e.g., phenol/formaldehyde resin) because of the toxicity of formaldehyde.[10] Therefore, studies of their pot life, curing kinetics, and kinetic parameters are topics of great interest, and the optimization of the manufacturing processes is of great importance.[11] In some specific applications, a long pot life is needed to mix PFA resin and acid catalysts to satisfy convenient handling and processability parameters.[12]

The curing of PFA resins and their blends and composites has been studied previously in the presence of several Brønsted acid catalysts, including organic acids, such as *p*-toluene sulfonic acid,[2,13] oxalic acid (OX),[14] maleic anhydride[3,5,15]; mineral acids, such as phosphoric acid[15] and sulfuric acid;[16] and Lewis acids, such as ferric chloride hexahydrate,[15] $TiCl_4$, $SnCl_4$,[7] and $ZnCl_2$;[17] and iodine.[14] The curing mechanism of FA in the presence of acid catalysts involves two steps:

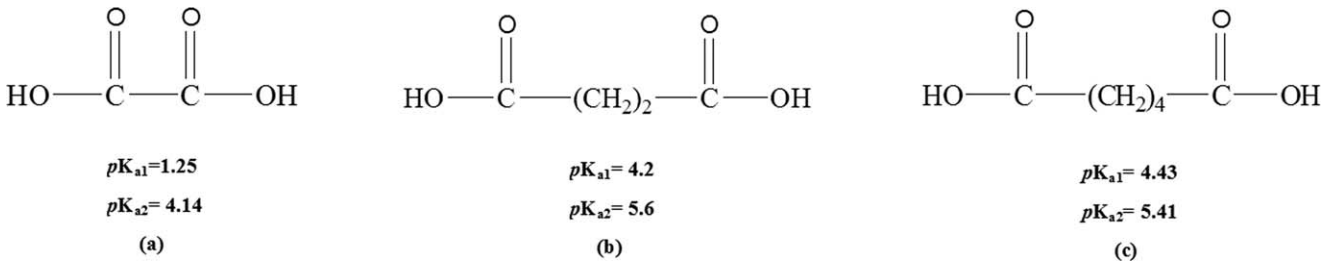

Figure 1. Chemical structures of (a) OX (pK_{a1} = 1.25, pK_{a2} = 4.14), (b) SU (pK_{a1} = 4.2, pK_{a2} = 5.6), and (c) AD (pK_{a1} = 4.43, pK_{a2} = 5.41).

1. The condensation reaction of a methylol group with the C5 position of another furan ring, which causes dehydration.
2. The crosslinking of the linear oligomers, which leads to black-colored networks.[7,18,19]

It has been demonstrated[7,19] that the hydrogen atoms positioned on the methylene bridge between two furan rings play an important role in the color formation and are responsible for the crosslinking reaction with hydroxyl end groups of another chain. The other suggested mechanism for PFA crosslinking is the Diels–Alder cycloaddition between the furan rings (diene) in oligomeric molecules and the conjugated dihydrofuranic sequences (dienophile).[7,18]

Two major factors affecting the curing rate of PFA resins are the type and concentration of acid catalyst used. The application of a weak acid catalyst, such as acetic acid, leads to the incomplete curing of the resin even at temperatures higher than 100 °C. However, PFA usually reacts at a very high rate in the presence of strong mineral or organic acids; this leads to instantaneous curing reactions. In the presence of mild acids, such as maleic anhydride or OX, resins are cured at lower rates.

The curing kinetics of PFA resin have been previously studied in the presence of maleic anhydride[5] or strong acid catalysts, such as *p*-toluene sulfonic acid.[2] So, in this study, the curing kinetics and pot life of PFA resins catalyzed in the presence of a homologous series of weak dicarboxylic acids differing in their catalytic power were investigated. This study provided us with a chance to modulate the extent and rate of resin curing reactions intended for special applications where there is a need to prevent premature curing during the fabrication process. The curing kinetics were determined with differential scanning calorimetry (DSC) and frequency-sweep rheometry at 0, 6, and 24 h after the addition of the dicarboxylic acid catalysts, that is, OX, succinic acid (SU), and adipic acid (AD). The results were thereafter confirmed by the gas chromatography/mass spectrometry (GC/MS) data of gaseous molecules evolving from the PFA/OX mixture during curing.

EXPERIMENTAL

Materials

FA [molecular weight (MW) = 98.10 g/mol, boiling point = 170 °C], maleic anhydride (MW = 98.06 g/mol, melting point = 51–56 °C), OX (MW = 90.03 g/mol, purity > 99%), SU (MW = 118.09 g/mol, purity > 99%), and AD (MW = 146.1412 g/mol, purity >99%) were purchased from Merck Chemical Co. (Darmstadt, Germany). The chemical structures of the acid catalysts are illustrated in Figure 1. All other solvents and reagents were analytical grade and were used as received. Deionized water was prepared in house by reverse osmosis with an AquaMAX Ultra water-purification system (Younglin, Ultra 370 Series, South Korea).

PFA Synthesis

The acid-catalyzed synthesis of the PFA resin was carried out in a three-necked, round-bottomed reaction flask equipped with a water-cooled reflux condenser, a thermometer, and a stirrer on the basis of the procedure originally described by Schmitt[9] and Wewerka *et al.*[20] To this end, maleic anhydride was totally dissolved in a definite volume of deionized water and mixed with the FA aqueous solution at a FA/water/maleic anhydride weight ratio of 112:40:0.2 under vigorous stirring. Thereafter, the flask was heated to the FA–water azeotrope temperature (92 °C) in an oil bath and held at the same temperature for 30 min. Thereafter, the reaction mixture was cooled down to 50 °C by immersion of the flask in an ice–water bath. The pH of the mixture was adjusted to 7 through the addition of a few droplets of NaOH solution (1.25 *N*). A saturated NaCl solution was used to break down the resulting emulsion after neutralization. The aqueous phase was separated, decanted, and disposed. Finally, the residual water was removed from the polymer-rich phase via vacuum rotoevaporation at 90 °C and 212.8 mbar. Table I summarizes some of the important characteristics of the synthesized resins.

Characterization

The curing behavior of the PFA resin was studied with DSC on a Mettler-Toledo DSC 1 instrument. Temperature and enthalpy calibrations were carried out with mercury, indium, tin, lead, and zinc standards. A definite sample weight was placed into the sealed aluminum pans. DSC measurements were performed under a nitrogen atmosphere from 25 to 350 °C at heating rates of 5, 6.5, 8.5, and 10 °C/min. Isothermal DSC measurements were conducted at a constant temperature of 100 °C for PFA resins containing 1, 2, and 3 wt % OX to determine the optimal concentration of the curing catalyst. These formulations were coded as PFA/1OX, PFA/2OX, and PFA/3OX, respectively. The curing parameters of PFA/3OX were evaluated 0, 6, and 24 h after the

Table I. Characteristic Properties of the Synthesized PFA Resin

η (Pa s)	PDI	M_w (g/mol)	M_n (g/mol)
150	1.8	1064.6	579.57

M_w, weight-average molecular weight; M_n, number-average molecular weight; PDI, polydispersity index.

Table II. Formulations and Sample Coding for the Rheological and DSC Measurements

Acid catalyst	Time after mixing (h)		
	0	6	24
OX	PFA/OX0	PFA/OX6	PFA/OX24
SU	PFA/SU0	PFA/SU6	PFA/SU24
AD	PFA/AD0	PFA/AD6	PFA/AD24

PFA stands for the PFA resin. The digit number shows the time interval (hours) after the catalyst addition.

addition of OX to PFA with three model-free isoconversional methods, that is, the Ozawa–Flynn–Wall (OFW), Kissinger–Akahira–Sunose (KAS), and Vyazovkin (VA) methods. These models have been previously validated in many cases to study the kinetics of the curing reactions of different thermosetting resins.[21–23]

Oscillatory rheological measurements were carried out in frequency-sweep mode with parallel-plate geometries (25-mm diameter and 0.05-mm gap) with an MCR300 rheometer (Anton Paar, Graz, Austria) operating under ambient conditions for PFA resin samples containing 3 wt % acid catalyst 0, 6, and 24 h after the addition of the catalyst. The investigated formulations are presented in Table II. The range of frequencies was set from 0.01 to 1000 Hz at an oscillation amplitude of 1% strain. The linear viscoelastic range of the material was previously determined with the corresponding strain sweep tests.

The viscosity of the PFA/1OX, PFA/2OX, and PFA/3OX specimens over time was measured with a Brookfield viscometer (Selecta, VISCO STAR-R, Barcelona, Spain) at 25 °C.

Headspace gas chromatography separations were conducted with a CP-3800 Varian GC/MS instrument (Agilent Technologies, Santa Clara, CA) equipped with a wall-coated open tubular fused-silica capillary column (Varian, VF, 5-ms stationary phase, 30-m column length, 0.25-mm *i.d.*, 0.39-mm *o.d.*, 0.25-mm film thickness) at a 1 mL/min helium flow rate. The samples were heated to 180 °C; thereafter; the headspace gas phase was introduced into the column at a 1:20 split ratio. The initial temperature of the column was set at 50 °C; the temperature was held for 2 min, then increased at a rate of l0 °C/min to 250 °C, and held for 10 min. Analyte species were detected with a Saturn 2200 Varian mass spectrometer (10–650 m/z).

Theoretical Calculations

DSC Models. The real rates of the reactions, for example, that of the curing of thermoset resins, could not be directly inferred from the thermal analysis data, but a lot of information on the curing mechanism could be obtained by studying of the dependence of the effective activation energy (E_a) on the degree of conversion, or the degree of curing (α). Different models could be fitted to the DSC data to determine the corresponding dependency of E_a versus α. This demonstrated that the E_a versus α chart reflects the curing reaction kinetics.[24] The nonisothermal kinetics of a model process; composed of consecutive reactions, are discussed in this section.

The interpretation and inference of the chemical kinetics on the basis of methods with a single heating rate have been shown to have many shortcomings;[25,26] therefore, isoconversional methods based on multiple heating rates (i.e., *model-free kinetics methods*), for example, OFW,[27,28] KAS,[29,30] and VA methods,[31] have been used more recently. In these methods, the curing rate at a given α depends only on the temperature.[32] The equations governing the OFW and KAS methods are given in eq. (1) and eq. (2), respectively:

$$\log\ \beta = \log\left(\frac{AE_a}{R}\right) - \log[g(\alpha)] - 2.315 - 0.4567\frac{E_a}{RT_\alpha} \quad (1)$$

$$\ln\left(\frac{\beta}{T_\alpha^2}\right) = \ln\left[\frac{AR}{E_a g(\alpha)}\right] - \frac{E_a}{RT_\alpha} \quad (2)$$

$$g(\alpha) = \int_{\alpha_0}^{\alpha} \frac{1}{f(\alpha)}\,dx \quad (3)$$

where T_α is the temperature for a certain α, β is the heating rate, α_0 is the initial degree of curing, and $g(\alpha)$ is a function of α. The plotting logβ versus $1/T$ at any α leads to $-(0.4567E_\alpha/R)$ for the slope of the line based on the OFW method. In the KAS method, E_a of the reaction can be obtained from the slope of the plot of β/T_α^2 versus $1/T_\alpha$.

VA[31] developed an advanced model that performs integrations over small conversion intervals ($\Delta\alpha \approx 0.01$). Then, for a set of n experiments performed at different heating rates $[T_i(t)]$, E_a is determined at any particular α as the value that minimizes the function given by eq. (5), that is, $\Phi(E_a)$. Systematic errors associated with major integrations are minimized in this method[31]:

$$[E_a, T(t_\alpha)] = \int_{t_\alpha - \Delta\alpha}^{t_\alpha} \exp\left[\frac{-E_a}{RT(t)}\right] \quad (4)$$

$$\Phi(E_a) = \sum_{i=1}^{n}\sum_{j\neq 1}^{n} \frac{J[E_a, T_i(t_\alpha)]}{J[E_a, T_j(t_\alpha)]} \quad (5)$$

Rheology Models. The simple power law model can be used to describe the rheological behavior of gels through the determination of the critical gel parameters, where the dynamic moduli are related as follows:[33,34]

$$G'(\omega) = \frac{S\pi\omega^n}{2\Gamma(n)\sin\left(\frac{\pi n}{2}\right)} \quad (6)$$

$$G''(\omega) = \frac{S\pi\omega^n}{2\Gamma(n)\cos\left(\frac{\pi n}{2}\right)} \quad (7)$$

where S is the gel strength or stiffness parameter, which depends on the crosslinking density and chain flexibility of the parent chains; $\Gamma(n)$ is the gamma function; and n is the relaxation exponent. When n is 1, the material is purely viscous, and when n is 0, the material is purely elastic. Chambon and Winter[34] assumed that the case when n is 0.5 could be considered an ideal gel.

Weak gels behave like three-dimensional networks with limited flowability and a finite relaxation time.[35] Gabriele *et al.*[36]

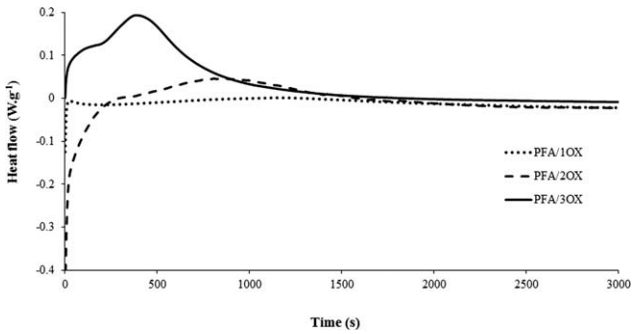

Figure 2. DSC thermograms of the heat release during the isothermal curing of PFA/1OX, PFA/2OX, and PFA/3OX at 100 °C.

proposed a model describing weak gels, suggesting that the gel structure corresponds to a cooperative arrangement of flow units forming interacting strands. In this model, during dynamic oscillatory experiments, the coordination parameter (z) is the number of rheological units interacting with each other in a three-dimensional structure, whereas gel strands may be considered a combination of flow units. The complex modulus (G^*) is described by the following equation:

$$G^*(\omega) = \sqrt{G'(\omega)^2 + G''(\omega)^2} = A_F \omega^{1/z} \quad (8)$$

where A_F is the gel strength or the strength of the interactions between the flow units. This equation provides useful information about the rheological structure of a three-dimensional network where flow units are linked by more or less strong interactions. When the loss modulus (G'') is small [$G'' \ll$ Storage modulus (G')], $G^* \approx G'$, the model can be expressed as follows:

$$G'(\omega) = A_F \omega^{1/z} \quad (9)$$

RESULTS AND DISCUSSION

DSC Measurements

To optimize the OX catalyst concentration for the curing of the PFA resin, isothermal DSC measurements were carried out at 100 °C on PFA/1OX, PFA/2OX, and PFA/3OX samples (Figure 2). The results demonstrate a higher enthalpy for the curing reaction in PFA/3OX (130.78 J/g) than in PFA/2OX (59.05 J/g) or PFA/1OX (17.05 J/g) OX. Hence, PFA/3OX samples were used for the nonisothermal DSC studies.

The characterization of the curing process for the PFA resin was carried out with nonisothermal DSC analyses at 0, 6, and 24 h after the addition of a corresponding acid catalysts to the resin; their related DSC thermograms are illustrated in Figures 3–5. Tables III and IV present the heat released during the nonisothermal curing of PFA. The DSC results for the PFA/SU and PFA/AD mixtures showed slight peaks at different heating rates and time intervals (Figures 3 and 4). The range of curing temperatures is presented in Table III. According to the results (Table III), less heat was released from the PFA/SU and PFA/AD mixtures because SU (pK_{a1} = 4.2, pK_{a2} = 5.6) and AD ($pK_{a\ 1}$ = 4.43, $pK_{a\ 2}$ = 5.41) were weak acids compared to OX. Nevertheless, as the SU dissociation was greater than that of AD, the heat released from the PFA/SU mixtures was greater than that released from the PFA/AD mixture at any time point during the reaction. Moreover, the heat released from these samples increased with passing time from 0 to 24 h. Because of their lower dissociation constants and acidity, we supposed

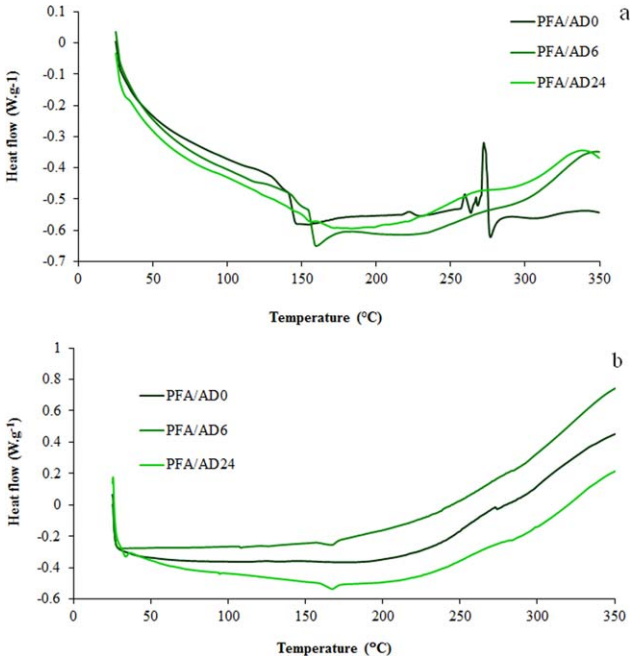

Figure 3. DSC thermograms of PFA resins containing 3 wt % AD (PFA/AD0, PFA/AD6, and PFA/AD24) at different heating rates: (a) 5 and (b) 10 °C/min. [Color figure can be viewed in the online issue, which is available at wileyonlinelibrary.com.]

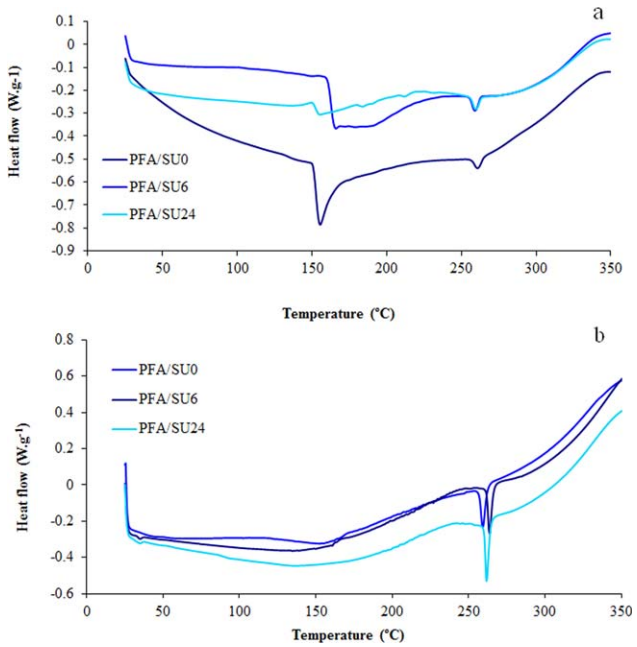

Figure 4. DSC thermograms of PFA resins containing 3 wt % SU (PFA/SU0, PFA/SU6, and PFA/SU24) at different heating rates: (a) 5 and (b) 10 °C/min. [Color figure can be viewed in the online issue, which is available at wileyonlinelibrary.com.]

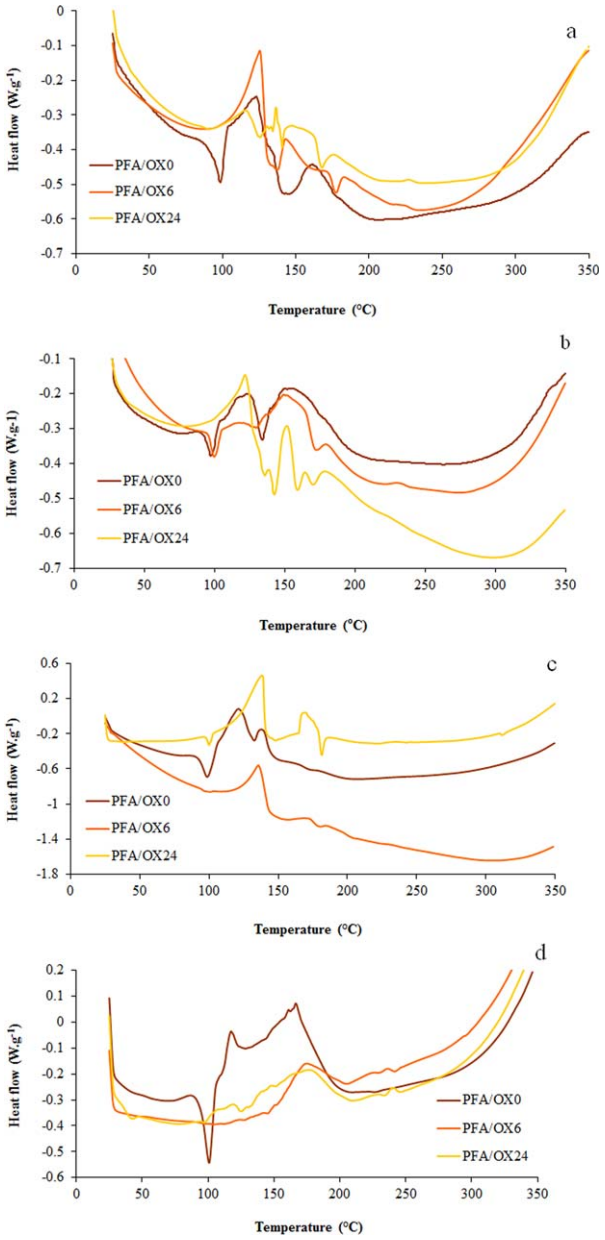

Figure 5. DSC thermograms of PFA containing 3 wt % OX (PFA/OX0, PFA/OX6, and PFA/OX24) at different heating rates: (a) 5, (b) 6.5, (c) 8.5, and (d) 10 °C/min. [Color figure can be viewed in the online issue, which is available at wileyonlinelibrary.com.]

that the ionization, catalytic activity, and miscibility of SU and AD was inherently limited in the resin matrix. Nevertheless, these characteristics were improved with passing time from the starting point of mixing. The rheology results confirmed these postulates because the viscosity of the systems is reduced as a function of the reaction time. This phenomenon was attributed to the plasticizing effects exerted by SU and AD curing agents.

Nonisothermal DSC results for PFA/OX mixtures showed two peaks at time 0, and the intensity of the peaks increased as a function of time (Figure 5). The peak temperatures are shown in Table IV. Milkovic *et al.*[37] also observed two peaks for the curing of FA catalyzed with *p*-toluene sulfonic acid. These two stages were attributed to the extension of the polymerization reaction and were followed by a distinct step of crosslinking. The condensation and crosslinking reactions of FA and FA with tris(Z-hydroxyethyl)isocyanurate were previously described by Xue-Si *et al.*[38] They observed four exothermic peaks in DSC thermograms during the thermal condensation of FA and FA with tris(*Z*-hydroxyethyl)isocyanurate in the presence of sulfuric acid. They suggested that these peaks, including I, II (50–80 °C), III (110–130 °C), and IV (150–190 °C), were related to the linear polycondensation of FA via head-to-tail condensation, head-to-head etherification, a crosslinking dehydration reaction between the methylene group and terminal hydroxyl group of FA polymeric chains, and a further crosslinking reaction at a higher temperature, respectively. In this study, FA was already polymerized to PFA; thus, there was more possibility for crosslinking in comparison to in the partial polymerization of the resin during DSC experiments. Moreover, the acid catalyst used for PFA curing, that is, OX ($pK_{a\ 1}$ = 1.25, $pK_{a\ 2}$ = 4.14), is a weak acid compared to *p*-toluene sulfonic acid and so on. So, the curing reaction of the resin in the presence of OX shifted to higher temperatures, about 100–200 °C, where low-molecular-weight components may have evaporated. Thus, with increasing temperature in the mixture, two processes occurred, that is, resin curing, which was an exothermic reaction, and the evaporation of low-molecular-weight components and water (as a condensation reaction byproduct), which was an endothermic reaction. The existence of the two exothermic and endothermic reactions proved the appearance of more than one peak in the DSC thermograms.

The heat flow data were processed to obtain the fractional conversion (α) and the rate of reaction ($d\alpha/dt$) under the

Table III. Heat of Polymerization (J/g) and Curing Temperatures of PFA Resins Containing 3 wt % SU and AD at Different Heating Rates and Times

$T_{onset} - T_{endset}$ (°C)		Heating rate		
10 °C/min	5 °C/min	10 °C/min	5 °C/min	Formulation
160.34-253.9	191.08-254.19	4.09	8.085	PFA/SU0
147.87-263.4	195.11-254.37	5.4	18.48	PFA/SU6
144.24-262.17	185.51-254.84	5.84	24.774	PFA/SU24
133.13-163.53	151.85-209.97	0.96	3.69	PFA/AD0
127.69-162.64	161.23-181.42	1.44	9.52	PFA/AD6
—	156.58-168.66		0.594	PFA/AD24

Table IV. Heat of Polymerization and Curing Temperatures of the PFA/3OX at Different Heating Rates and Times

T_{peak} (°C)										ΔH_{total} (J/g)			Heating rate (°C/min)
PFA/OX24			PFA/OX6				PFA/OX0			PFA/OX24	PFA/OX6	PFA/OX0	
T_{p4}	T_{p3}	T_{p2}	T_{p1}	T_{p4}	T_{p3}	T_{p2}	T_{p1}	T_{p2}	T_{p1}				
176.6	159	136.6	115.87	183.4	170.74	143.4	125.61	162.02	123.39	67.73 (α = 0.2091)	68.05 (α = 0.2054)	85.644	5
178.6	164.32	151.7	121.9	232	180.6	152.4	117.06	155.88	123.6	105.395	57.127 (α = 0.398)	94.897	6.5
235	189.05	169.95	138.27	—	186.23	171.86	135.67	137.65	121.38	133.83	61.949 (α = 0.4722)	117.378	8.5
239.8	225.8	175.06	118.35	—	235.4	217.87	174.08	166.21	117.71	69.718 (α = 0.09811)	20.488 (α = 0.7349)	77.303	10

α was determined at a certain time at ambient temperature.

assumption that the heat flow was proportional to the reaction rate. For an exothermic reaction, eq. (10) was applied:

$$\frac{dH}{dt} \approx -\frac{d\alpha}{dt} \tag{10}$$

The partial conversion was calculated by the residual curing enthalpy obtained from dynamic DSC scans according to Hardis *et al.*[39] with the application of eq. (11):

$$\alpha = \frac{\Delta H_T - \Delta H_R}{\Delta H_T} = \frac{\Delta H}{\Delta H_T} \tag{11}$$

where ΔH_R is the residual reaction heat of a sample partially cured for a specific time at 25 °C as measured by a dynamic DSC scan and ΔH_T is the total heat of the reaction evolving in a dynamic DSC scan directly after the mixing of the components ($t = 0$). The partial conversion results for PFA containing OX are presented in Table IV. Because of the higher amount of heat released for PFA/OX24 compared with PFA/OX0, the partial α for PFA/OX24 could not be calculated.

The results of the curing degree for PFA/OX6 (partial conversion) with the application of eq. (11) are also presented in Table IV. We expected that there would be an increase in α with increasing reaction time; thus, the calculated curing enthalpy from the DSC measurements had to be reduced. The curing enthalpy decreased from 0 to 6 h and then increased to 24 h. We assumed that the enthalpy would decrease after 6 h because of the partial curing of the resin, but the increase between 6 and 24 h due to the corresponding increase in the viscosity of the mixture was supported by our laboratory observations. In other words, gelation occurred during this period of time, and consequently, the mobility of high-molecular-weight chains became limited. In this situation, the motions of the low-molecular-weight chains were not affected. Thus, with increasing time from 6 to 24 h, the amount of low-molecular-weight chains decreased, and with increasing temperature in the DSC measurements performed at 24 h, the amount of endothermic evaporation decreased. So, the total heat released from this sample was increased.

According to the results, no considerable curing occurred at ambient conditions when weak dicarboxylic acids such as OX (in contrast to their strong counterparts, e.g., *p*-toluene sulfonic acid) were used as curing agents; this provided more time for the operator to fabricate bulky parts, for example, by making thermosetting composite materials by hand layup.

The DSC data were used to evaluate the dependence between the apparent E_a and α (E_a–α), as illustrated in Figures 6 and 7. On the basis of this dependence, we concluded that the acid-catalyzed curing of PFA followed a multistep kinetics pattern expressed by variations observed in the E_as at different degrees of curing. The results obtained from eqs. (1) and (2) were similar to those illustrated in Figure 6.

For the PFA/OX0 compositions, at the beginning of the reaction, where $\alpha < 0.05$, a slight increase in the E_a values from 67 to 119 kJ/mol was observed; this was attributed to the formation of the active species in the early stage of the condensation reaction and the accumulation of reaction intermediates. With

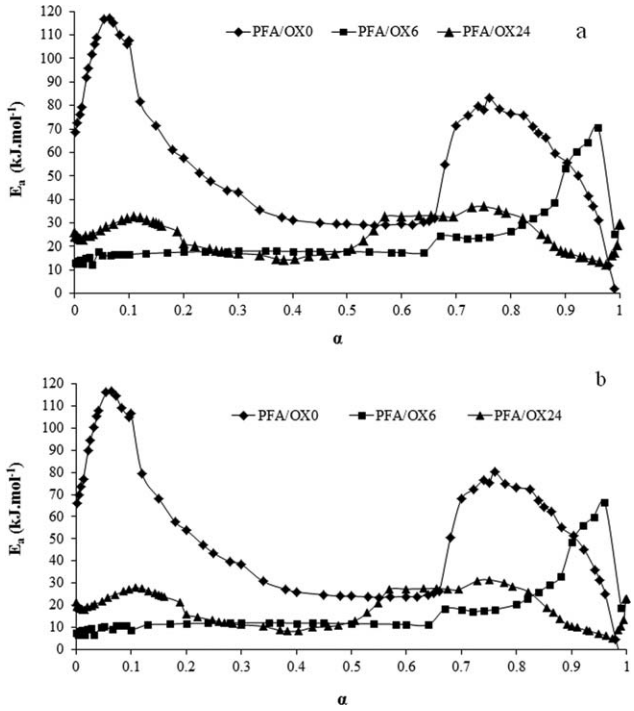

Figure 6. (a) OFW and (b) KAS E_as as a function of α for PFA/0OX, PFA/OX6, and PFA/OX24.

further development of the curing process, the intermediates were consumed, and the accumulation of these intermediates stopped.[24] Guigo *et al.*[5] also reported the same behavior in the study of FA monomer curing, whereas Domínguez *et al.*[2] reported it for PFA curing catalyzed with *p*-toluene sulfonic acid. Because PFA/OX6 and PFA/OX24 had adequate time for the formation of the carbenium active center, their initial E_a was low in comparison to that of the PFA/OX0 samples. After this stage, until α was 0.65, the E_a values were about 30 kJ/mol and quasi-constant; this suggested the domination of a single reaction in this range of αs.[24,40]

For $0.65 < \alpha < 0.76$, E_a increased to 80 kJ/mol; this represented a change in the reaction mechanism. The observed increase in E_a could have been due to the contribution of further crosslinking reactions.

For the PFA/OX6 composition, a constant E_a in the range of 18 kJ/mol was obtained (Figure 6) until α was 0.64; this indicated that the process could be approximated as a single reaction.[2,24] We assumed that the predominant reaction in this stage was a polycondensation reaction between PFA chains. As shown in Figure 6, for all formulations, E_a started to decrease at the final stage ($\alpha > 0.8$ for PFA/OX0 and OX24, $\alpha > 0.96$ for PFA/OX6). In the late curing stage and in the glassy state, chains with higher molecular weights became frozen in their positions; this resulted in a cessation of the reaction, and the mobility of the polymer chains was severely limited. Thus, the rate of the curing reaction was controlled by the diffusion of unreacted, residual functional groups and small chains and molecules present in the system. The diffusion control process resulted in a decrease in E_a.[2,41] In other words, vitrification caused a dramatic reduction in the molecular mobility, and this led to a reduction in E_a at high degrees of curing.[5]

For PFA/OX24 at $\alpha < 0.2$, E_a was higher than what was calculated for PFA/OX6 because of the higher viscosity of the resin and limitations occurring in the mobility of the polymer chains compared to the PFA/OX6 samples. For PFA/OX24, an increase in E_a due to the crosslinking reaction started at $\alpha > 0.49$; this occurred earlier than the increases for PFA/OX0 and PFA/OX6 and indicated the progression of the curing reaction for the PFA/OX24 samples at ambient temperature for a duration of 24 h. Moreover, because of the reduction of low-molecular-weight components in the same formulation, a dramatic reduction in E_a was not observed in the diffusion-controlled stage ($\alpha > 0.9$). However, the PFA/OX0 and PFA/OX6 compositions exhibited a sharp reduction in E_a at $\alpha > 0.9$. and the VA model for PFA/OX6 (Figure 7) was in line with the OFW and KAS models, but the model could not anticipate the PFA/OX0 and PFA/OX24 behavior. In this method, for PFA/OX0 and PFA/OX24, the amount of E_a in some curing degrees gave a negative value, which was not true as E_a.

Rotational Viscometry

The viscosity of PFA/3OX increased after about 330–340 min; this time period was considered the gelation time (t_{gel}; Figure 8). These results confirmed our suggestion about the DSC data after 6 and 24 h. As expected, the gelation time for the two other systems (PFA/1OX and PFA/2OX) increased to about 440 and 1100 min, respectively, because of the reduction in the OX concentration (C_{OX}). These results are presented in Table V and fit the exponential decay first-order model in the following equation:

$$t_{gel} = 792 \times \exp(-C_{OX}/0.56) + 308 \quad (R^2 = 1) \qquad (12)$$

GC/MS Analysis

GC/MS analysis was also performed to confirm DSC findings. The dimer/monomer and trimer/monomer ratios were calculated from GC/MS spectra of PFA/OX0, PFA/OX6, and PFA/OX24, as shown in Table VI. The level of dimer/monomer values increased significantly with increasing time from 0 to 6 h. The amount of dimer increased with increasing extent of the reaction of monomers to their higher counterparts, including dimers. Thus, the amount of monomer was significantly reduced after 6 h, and the dimer/monomer ratio for the PFA/

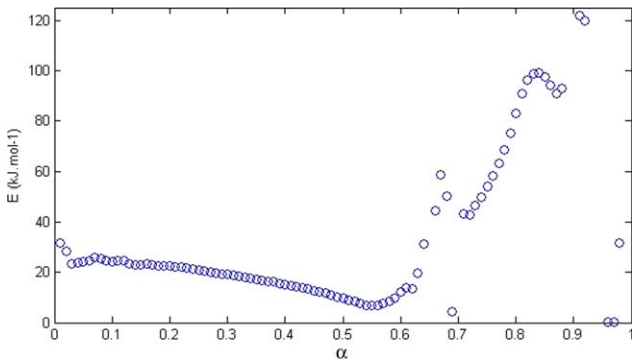

Figure 7. VA E_a as a function of α for PFA/OX6. [Color figure can be viewed in the online issue, which is available at wileyonlinelibrary.com.]

Table V. Gel Time (Pot Life) for PFA/1OX, PFA/2OX, and PFA/3OX at Ambient Temperature

Formulation	PFA/3OX	PFA/2OX	PFA/1OX
Gel time (min)	330	440	1100

OX24 samples was reduced to 5.963, whereas change in the trimer/monomer was not comparable. These results confirm that with increasing time after the addition of a catalyst up to 24 h, the viscosity of the resin increased because of the progression of the curing system.

Frequency-Sweep Analysis

The rheological measurements were carried out to investigate viscosity changes during the curing reactions of the resin. As shown in Figures 9–11, the modulus and viscosity of the resin significantly increased when the acid catalyst was added at a time of 0 h. Nevertheless, these increases could not be attributed to the curing of the resin in the presence of acids because AD and SU were weak acids and could not induce curing at room temperature. Thus, we assumed that the behavior was due to the nondissolved and nonionized acids acting as filler particles at this time. For these samples, G' exhibited a plateau and frequency-independent behavior; this indicated that the elastic behavior of the suspensions was strengthened. Nobile and Raimondo[42] also observed this behavior for epoxy–amine resin/carbon nanofiber dispersions and attributed it to the interconnected structures of the fillers.

At the beginning of the test run (t = 0 h), the modulus and viscosity values were almost similar for three systems, and with a further increase in the time (t = 6 h), the values for the PFA/SU and PFA/AD systems decreased slightly compared with that of the PFA/OX sample. A slight decrease in the modulus and viscosity values was attributed to the dissolving and/or partial ionization of the catalysts and the reduction of filler effects. The rheological findings for the PFA/SU24 and PFA/AD24 samples demonstrated significant decreases in the modulus and viscosity values due to the increase in the miscibility of these acids with the resin acting as a plasticizer, as previously mentioned. The amount of this reduction was similar at 6 h because of the similar and lower acidity of the two acids. However, after 24 h, the higher acidity constant for SU affected G' and the viscosity

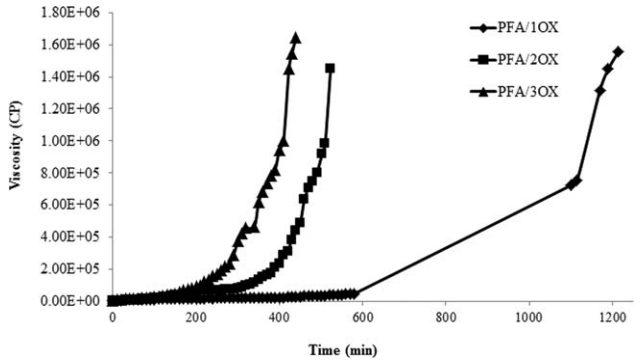

Figure 8. Relationship between viscosity and time for resins containing PFA/1OX, PFA/2OX, and PFA/3OX at the ambient temperature.

Table VI. Evaporated Phase Component Obtained from GC/MS Results

Formulation	Monomer	Component ratio: Dimer/ monomer	Dimer (ether)/ monomer	Trimer/ monomer
PFA/OX0	1	4.358	2.562	1.784
PFA/OX6	1	27.3934	4.008	2.766
PFA/OX24	1	3.605	2.358	2.164

values for PFA/SU24 (573 Pa, 29,100 Pa s); this was higher than that of PFA/AD24 (0.0467 Pa, 15 Pa s). According to the findings shown in Figures 9 and 10, the effect of AD on the viscosity reduction was greater than the presence of SU; this indicated a higher miscibility of AD with the resin in comparison to that of the SU/resin compositions. This was due to the longer length of the methyl backbone chain and the greater hydrophobicity of AD compared to that of SU. This induced a greater interaction

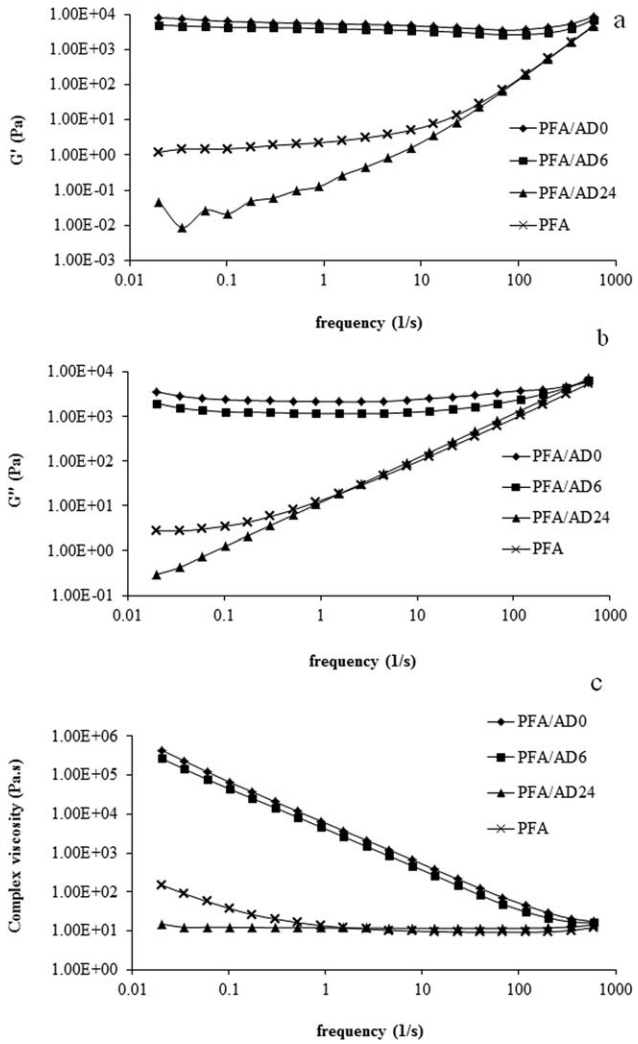

Figure 9. Frequency dependence of the (a) G', (b) G'', and (c) complex viscosity for PFA/AD0, PFA/AD6, and PFA/AD24.

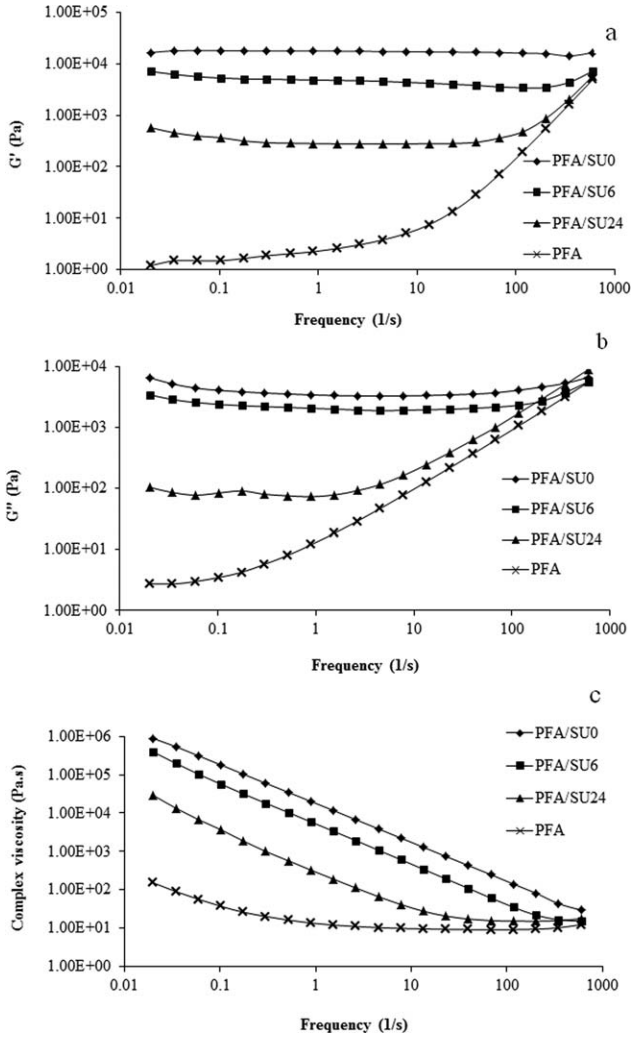

Figure 10. Frequency dependence of the (a) G', (b) G'', and (c) complex viscosity for PFA/SU0, PFA/SU6, and PFA/SU24.

of AD with the hydrophobic PFA resin. Thus, the friction between the resin chains and viscosity was reduced.

A neat PFA resin is not a completely Newtonian fluid, and its viscosity is dependent on the frequency. Ibnyaich[43] also observed this behavior for FA resin. Shear thinning behavior, a decrease in the viscosity with an increase in the shear rate/frequency, was observed in all of the formulations except PFA/AD24. In PFA/AD24, η^* decreased sharply with a corresponding increase in the frequency and reached a value equal to that of the pure resin. This indicated Newtonian behavior for the compound at a higher frequency and a fluid rather than filler dominating fluid dynamics. The acidity of SU and AD is low, so the curing resulting from them was not sensible compared to their plasticizing effect.

Moreover, as illustrated in Figure 11, the values of the modulus and viscosity for PFA/OX did not change (23,500 Pa, 1.30×10^6 Pa s). This behavior was expected because the acidity constant of OX was higher than the values for SU and AD. On the other hand, because of the higher polarity and hydrophilicity of OX, its interaction and miscibility with the PFA resin were lower than those for SU and AD with the resin. Thus, OX could not act and could not be considered a plasticizer. As shown in Figure 11, there was an apparent plateau of G' versus the frequency at the three time points studied here. This indicated a pseudo-solidlike behavior of the formulation. PFA/AD0, PFA/SU0, PFA/AD6, and PFA/SU6 in a relatively low-frequency region ($<200\ s^{-1}$) also exhibited the same behavior.

The crossing point of the G' and G'' curves is a criteria for indicating a change from viscous liquid to elastic solid behavior.[44] For the neat PFA and PFA/AD24 samples in the low-frequency region, G' was lower than G'', whereas the increase in G' with increasing frequency was faster than that of G''; this led to the crossing of G' and G'' at a certain frequency ($600\ s^{-1}$), after which G' became higher than G''. This indicated that the formulations behaved as viscous liquids. In other formulations, G' was higher than G''; this indicated that the materials were elastic.

The results obtained by the fitting of the experimental results to the Winter and Chambon and Gabriele models are presented in

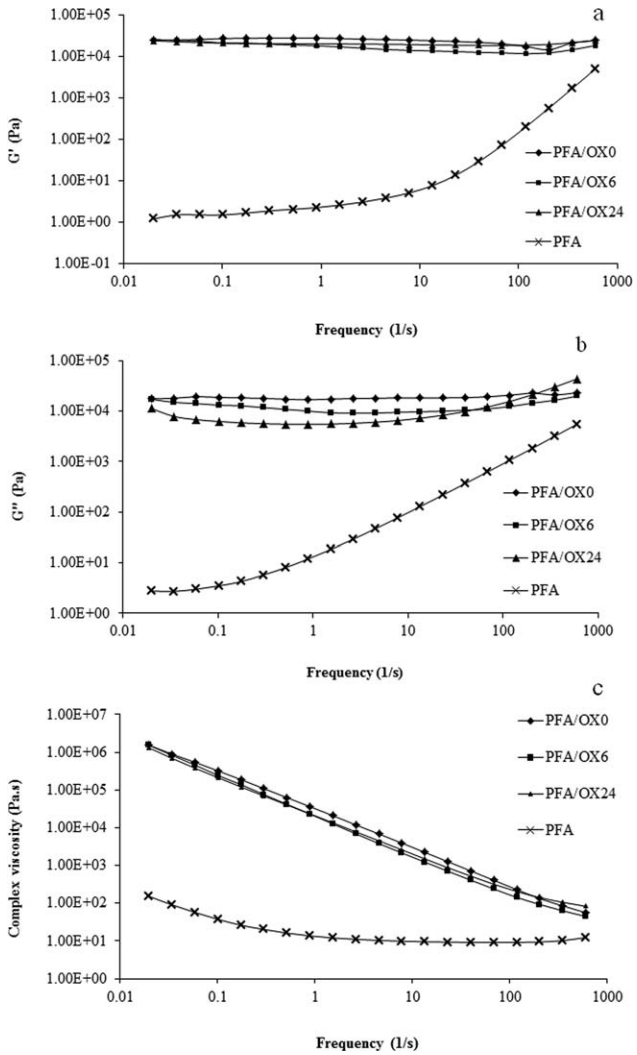

Figure 11. Frequency dependence of the (a) G', (b) G'', and (c) complex viscosity for PFA/OX0, PFA/OX6, and PFA/OX24.

Table VII. Model Parameters of the Winter and Chambon Models for the PFA/Acid Catalysts

Sample	n	s (Pa s^n)	R^2
PFA	1	5.43	0.999
PFA/OX24	0.6311	1377.8	0.98
PFA/SU24	1	8.98	0.999
PFA/AD0	0.084	2452.8	0.75
PFA/AD6	0.26	812.56	0.864
PFA/AD24	1	6.46	0.999

Tables VII and VIII, respectively. Both models were best fitted for the formulations after 24 h. This suggested that the acid catalysts at 0 and 6 h behaved like fillers, but after 24 h, gels were formed.

A comparison between the numerical values reported in Tables VII and VIII indicates a correlation between both parameters of the two models. The exponent in the Winter and Chambon model was the inverse of the coordination parameter in the Gabriele *et al.* model, whereas the gel stiffness was similar to the gel strength. Both series reflected analogous tendencies and showed that the stiffness and solidlike behavior of the formulation were enhanced with the acid strength.

The relaxation exponent for PFA/OX24 ($n = 0.63$) was lower than those of PFA/SU24 ($n = 1$) and PFA/AD24 ($n = 1$); this indicated solidlike behavior of PFA/OX24 and liquidlike behavior for the two later formulations. In addition, the relaxation exponent increased with time for the PFA/AD24 formulation; this reflected the plasticizing effect of AD on PFA with time progression and an increase in the liquidlike behavior of the formulation from 0 to 24 h.

The fitted equations (exponential decay, first order) for gel strength and gel stiffness as a function of the number of methylene groups of the acid catalysts could be expressed as follows:

$$S = 1371.34 \times \exp(2-C/0.317) + 6.46 \quad (R^2 = 1) \qquad (13)$$

$$A_F = 1938.62 \times \exp(2-C/0.318) + 5.38 \quad (R^2 = 1) \qquad (14)$$

CONCLUSIONS

In this study, the pot life of an FA resin was determined in the presence of three different homologous dicarboxylic acids, consisting of OX, SU, and AD. The DSC results show that the extent of curing in the presence of OX was higher than the same specimens containing either SU or AD. DSC and rheometry measurements also showed that no significant curing reactions occurred in the presence of SU and AD. These acids acted as plasticizers and reduced the modulus and viscosity values with increasing time from 0 to 24 h. GC/MS analysis of the gas phase evolved from the heated resin containing OX at three time points revealed that the low-molecular-weight components were reduced at 24 h upon curing. Furthermore, the E_a profile during curing was calculated with the model-free kinetics methods of KAS, OFW, and VA. The first two methods showed similar E_a profiles.

The rheological properties of the resin were modeled with the Gabriele *et al.* and Winter models. The obtained models' parameters were dependent on the type of acids and the time after mixing. Both series reflected analogous tendencies and showed that the stiffness and solidlike behavior of the formulations was enhanced with acid strength.

Table VIII. Model Parameters of the Gabriele Model for the PFA/Acid Catalysts

Sample	A_F (Pa $s^{1/z}$)	Z	R^2
PFA	—	—	—
PFA/OX24	1943.999	1.5586	0.96
PFA/SU24	9.037	0.9074	0.99
PFA/AD24	5.39	0.868	0.999

ACKNOWLEDGMENTS

This research was funded by the Iran Polymer and Petrochemical Institute (contract grant number 32751105). The authors are sincerely thankful for this financial support.

REFERENCES

1. Ciftci, H.; Öktem, Z.; Testereci, H. N. *Turk. J. Chem.* **2012**, *36*, 315.
2. Domínguez, J. C.; Grivel, J.-C.; Madsen, B. *Thermochim. Acta* **2012**, *529*, 29.
3. Guigo, N.; Mija, A.; Vincent, L.; Sbirrazzuoli, N. *Eur. Polym. J.* **2010**, *46*, 1016.
4. Assary, R. S.; Kim, T.; Low, J. J.; Greeley, J.; Curtiss, L. A. *Phys. Chem. Chem. Phys.* **2012**, *14*, 16603.
5. Guigo, N.; Mija, A.; Vincent, L.; Sbirrazzuoli, N. *Phys. Chem. Chem. Phys.* **2007**, *9*, 5359.
6. Huang, W.; Li, H.; Zhu, B.; Feng, Y.; Wang, S.; Zhang, S. *Ultrason. Sonochem.* **2007**, *14*, 67.
7. Choura, M.; Belgacem, N. M.; Gandini, A. *Macromolecules* **1996**, *29*, 3839.
8. Thoeni, A.; Baker, G.; Smith, C. *J. Cell. Plast.* **1971**, *7*, 294.
9. Schmitt, C. R. *Polym. Plast. Technol. Eng.* **1974**, *3*, 121.
10. Rivero, G.; Pettarin, V.; Vázquez, A.; Manfredi, L. *Thermochim. Acta* **2011**, *516*, 79.
11. Kang, J.; Wang, C.; Li, D.; He, G.; Tan, H. *Phys. Chem. Chem. Phys.* **2015**, *17*, 16519.
12. Jones Jr., J. W. "Latent Catalysts For Acid-Catalyzed Reactions". (**1967**), U.S. Pat. 3,317,474.
13. Renhe, H.; Hongmei, G.; Yaoji, T.; Qingyun, L. *Res. Dev.* **2011**, *5*, 161.
14. Song, C.; Wang, T.; Jiang, H.; Wang, X.; Cao, Y.; Qiu, J. *J. Membr. Sci.* **2010**, *361*, 22.
15. Wewerka, E. M.; Walters, K. L.; Moore, R. H. *Carbon* **1969**, *7*, 129.
16. Mokoena, T. T.; Ddamba, W. A. A.; Keikotlhaile, B. M. *South Afr. J. Chem.* **1999**, *52*, 2.

17. Sugama, T.; Kukacka, L. E. *J. Mater. Sci.* **1982**, *17*, 2067.
18. Zavaglia, R.; Guigo, N.; Sbirrazzuoli, N.; Mija, A.; Vincent, L. *J. Phys. Chem. B* **2012**, *116*, 8259.
19. Principe, M.; Ortiz, P.; Martínez, R. *Polym. Int.* **1999**, *48*, 637.
20. Wewerka, E. M.; Loughran, E. D.; Walters, K. L. *J. Appl. Polym. Sci.* **1971**, *15*, 1437.
21. Jovičić, M.; Radičević, R.; Budinski-Simendić, J. *J. Therm. Anal. Calorim.* **2008**, *94*, 143.
22. Pérez, J. M.; Oliet, M.; Alonso, M. V.; Rodríguez, F. *Thermochim. Acta* **2009**, *487*, 39.
23. Vertuccio, L.; Russo, S.; Raimondo, M.; Lafdi, K.; Guadagno, L. *RSC Adv.* **2015**, *5*, 90437.
24. Vyazovkin, S. *Thermochim. Acta* **1994**, *236*, 1.
25. Vyazovkin, S. *Thermochim. Acta* **2000**, *355*, 155.
26. Burnham, A. K. *Thermochim. Acta* **2000**, *355*, 165.
27. Ozawa, T. *Bull. Chem. Soc. Jpn.* **1965**, *38*, 1881.
28. Flynn, J. H.; Wall, L. A. *J. Polym. Sci. Part B: Polym. Lett.* **1966**, *4*, 323.
29. Jankovi, B. *AAPS PharmSciTech* **2010**, *11*, 103.
30. Akahira, T.; Sunose, T. *Res. Rep. Chiba Inst. Technol.* **1971**, *16*, 22.
31. Vyazovkin, S. *J. Comput. Chem.* **2001**, *22*, 178.
32. Vyazovkin, S.; Wight, C. A. *Thermochim. Acta* **1999**, *340*, 53.
33. Winter, H. H.; Chambon, F. *J. Rheol.* **1986**, *30*, 367.
34. Chambon, F.; Winter, H. H. *J. Rheol.* **1987**, *31*, 683.
35. Martínez-Ruvalcaba, A.; Rodrigue, D. *Carbohydr. Polym.*, **2007**, *67*, 586.
36. Gabriele, D.; deCindio, B.; D'Antona, P. *Rheol. Acta* **2001**, *40*, 120.
37. Milkovic, J.; Myers, G. E.; Young, R. A. *Cellul. Chem. Technol.* **1979**, *13*, 651–672.
38. Chen, X. S.; Zheng, G. D.; Liu, Z. H.; Xu, J. P. *Chin. J. Chem.* **1991**, *9*, 193.
39. Hardis, R.; Jessop, J. L.; Peters, F. E.; Kessler, M. R. *Compos. A* **2013**, *49*, 100.
40. Sbirrazzuoli, N.; Vyazovkin, S.; Mititelu, A.; Sladic, C.; Vincent, L. *Macromol. Chem. Phys.* **2003**, *204*, 1815.
41. Sbirrazzuoli, N.; Mititelu-Mija, A.; Vincent, L.; Alzina, C. *Thermochim. Acta* **2006**, *447*, 167.
42. Nobile, M. R.; Raimondo, M. *Polym. Compos.* **2015**, *36*, 1152.
43. Ibnyaich, A. M.S. Thesis, Luleå University of Technology, **2010**, p 60.
44. Zhu, J.; Wei, S.; Yadav, A.; Guo, Z. *Polymer* **2010**, *51*, 2643.